2-P

NASA TECHNICAL TRANSLATION NASA TT F-14425

GRATING-TYPE INFRARED FOURIER SPECTROMETER

M.N. Markov, V.I. Vedernikov, V.V. Ivanov, A.V. Kartashev and V.S. Petrov

Translation of "Bortovoy infrakrasnyy fur'ye-spektrmetr", Akademiya nauk SSSR. Fizicheskii Institut. Opticheskaya Laboratoriya, Moscow (Preprint No.189), 1969, 41 pages

NATIONAL AERONAUTICS AND SPACE ADMINISTRATION
WASHINGTON,D.C. 20546 JUNE 1972

GRATING-TYPE INFRARED FOURIER SPECTROMETER

by M. N. Markov, V. I. Vedernikov, V. V. Ivanov, A. V. Kartashev, and V. S. Petrov

From: Akademiya nauk SSSR. Fizicheskii Institut. Opticheskaya Laboratoriya, 1969. (Preprint no. 189) Moscow

41 pages

Physics Institute in the Name of P. N. Lebedev

Surprint No. 189

Optical Laboratory

M. N. Markov, et al

GRATING-TYPE INFRARED FOURIER SPECTROMETER

Moscow 1969

I. INTRODUCTION

In recent, scientific literature there appeared a large number of works devoted to the method of Fourier spectrometry. From the point of view of the theory of the method and its practical application, one can note works 1, 2, 3, 4, 5, 6.

Fourier spectroscopy has a series of important advantages in comparison to classic methods of recording the spectrum. However, there are also certain difficulties. Basically, these difficulties are related to the high sensitivity of the Fourier spectrometer to external mechanical interaction, rigid requirements, and to the quality of optical detail and mechanical nodes and finally, to the necessity of completing high-capacity mathematical operations on an IBM or special analogous converters for obtaining the usual optical spectrum.

From scientific literature there is information concerning the grating-type Fourier spectrometer for a region of the spectrum from 1.8 - 15 μm with a threshold resolution of 50 cm^{-1} [5]. However, a majority of instruments possess a rather large weight and overall size (25 kg and higher), which basically limits their areas of application in the framework of the laboratory experiments.

The purpose of our work was to produce a small-size Fourier spectrometer for the measurement of absolute spectral intensities of Earth emission and other planets in the wave-length range from 10 μm to 40 μm from aircraft, balloons, satellites and others.

II. GENERAL CORRELATION

There is sufficient information concerning the theory of the method, and therefore we will mention only briefly, the basic principles.

a) In the basis of the Fourier spectrometer there is classic schematic of an interferometer. Let us examine in the capacity of an example, one that is used more than others, which is the Michaelson interferometer.

The light source in this case is an aperture which is a parallel beam directed to the light-separator Π. Part of the beam, reflected by the light-divider is reflected from mirror Z_1, passes the light-divider and converges in

receiver B. The π part of the beam which is passed, is reflected from mirror Z_2, the light-divider and also focuses on the receiver. If mirrors Z_1 and Z_2 are situated symmetrically in relation to the plane of the light-divider, then the light waves from the source arrive at the receiver in phase, and we then observe a maximum signal. Motion difference may be obtained by shifting one of the mirrors. The relation of the signal in the receiver from the motion difference for multi-chromatic emission of wave-length λ has the following appearance:

$$S(\gamma) = Z(\sigma)\cos^2\pi\sigma\gamma = \tfrac{1}{2}B(\sigma)(1+\cos 2\pi\sigma\gamma) \tag{1}$$

where γ is the motion difference between beams, $\sigma = 1/\lambda$ is the emission frequency (cm^{-1}). If the source has a complex spectral composition, then the signal in the receiver will be

$$S(\gamma) = \tfrac{1}{2}\int_{\sigma_1}^{\sigma_2} Z(\sigma)(1+\cos 2\pi\sigma\gamma)\,d\sigma = \tfrac{1}{2}\int_{\sigma_1}^{\sigma_2} Z(\sigma)\cos 2\pi\sigma\gamma\,d\sigma + \Phi_0 \tag{2}$$

Part of the signal, depending on γ is designated by the interferogram

$$\Phi(\gamma) = \tfrac{1}{2}\int_{\sigma_1}^{\sigma_2} Z(\sigma)\cos 2\pi\sigma\gamma\,d\sigma \tag{3}$$

The unmodulated portion of the signal specificies the phon constant, whose quantity increases with an increase in the spectral interval $\Delta\sigma = \sigma_2 - \sigma_1$

$$\Phi_0 = Z(\sigma)\,\Delta\sigma \tag{4}$$

The optical spectrum $Z(\sigma)$ is related to interferogram $\Phi(\gamma)$ with a reverse Fourier conversion

$$Z(\sigma) = \int_0^{\gamma_{max}} \Phi(\gamma)\cos 2\pi\sigma\gamma\,d\gamma \tag{5}$$

where γ is the maximal motion difference.

b) The resolution capability of the Fourier spectrometer is determined by the maximal motion difference in the interferometer γ_{max}. Designating the.

interferogram $\Phi_{(\gamma)}$ as a cosine with a period λ_0, which corresponds to a monochromatic source, emitted on wave-length λ_0, and substituting in (5) we obtained a theoretical instrument function of the apparatus

$$Z(\sigma) = \frac{\sin 2\pi(\sigma-\sigma_0)\gamma_{max}}{2\pi(\sigma-\sigma_0)} \qquad (6)$$

the half-width of which is determined at the foundation by the first zero of function (6) (fig. 2) and is equal to

$$\delta\sigma = \frac{1}{2\gamma_{max}} \qquad (7)$$

Quantity $\delta\sigma$ is often determined as a theoretical threshold of instrument resolution.

c) Function (6) has a main maximum on frequency σ and secondary maximums located on frequency

$$\sigma_n = \sigma_0 \pm \frac{1+4n}{4\gamma_{max}} \qquad n=0,1,2...$$

The quantity of secondary maximums proportional to $\frac{4}{2\pi(1+4n)}$, and the quantity (minimum) located on frequency

$$\sigma_m = \sigma_0 \pm \frac{3+4m}{4\gamma_{max}} \qquad m = 0,1,2...$$

is proportional to $\frac{4}{2\pi(3+4m)}$.

It is easily seen that the dimensions of the first minimum compose approximately 20% of the main maximum, therefore the spectrum in the region of frequency σ may be severely distorted. For a decrease in dimensions of similar errors, the interferogram was multiplied by the function equal to 1 with $\gamma = 0$ and 0 with $\gamma = \gamma_{max}$, which is called a adjustment function. A similar procedure is called an "apodization." The appearance of the instrument function with a triangular adjustment function is shown in fig. 2.

It is easy to demonstrate that with the utilization of a triangular adjustment function, the resolution threshold of the instrument is equal to

$$\delta\sigma = \frac{1}{\gamma_{max}}$$

d) In the absence of classic, spectral instruments (prismatic, diffractionary, Fabry-Perot standard and others) in the Fourier spectrometer, the spectrum region is limited by the transparency of the utilized materials and the range of the emission receiver. With short-wave emission the spectrum region may be limited by the more rigid requirements on mechanical nodes of the apparatus and also by vibrations whose influence increases with wave length decrease in the tested spectrum. This is the reason why Fourier spectroscopy, at the present time, is more successfully utilized in long-wave portions of the spectrum ($\lambda \geq 10\,\mu$m).

e) Transmission

As in usual spectro-apparatus, the transmission of the Fourier spectrometer is determined by the admissibility of a given resolution capability and dimensions of the input aperture S and the solid angle Ω (fig. 1).

In physical terms such a limitation may be explained in the following manner. By observing the interferometer picture from the monochromatic source in a parallel beam from the receiver, we observe bonded bands of equal inclination, localized to infinity (in the input diaphragm). With an increase in motion difference, the number of the bands is increased. A limiting factor in a given dimension of the diaphragm is a motion difference γ_{max} (resolution capability) at which, in the input diaphragm, besides the central one, there appears a primary side-band. With this, the amplitude of the interferogram $\Phi_{(\gamma)}$ drops to 0 and further increase in motion difference does not contribute to resolution capability.

In work [7] there was obtained a correlation for the variable-composing flow in the receiver

$$\Phi(\gamma, \sigma_0) = B(\sigma_0)\Omega S \frac{\sin \pi\gamma\sigma_0 \Omega/2\pi}{\pi\gamma\sigma_0\Omega/2\pi} \cos 2\pi\sigma_0\gamma\left[1 - \frac{\Omega}{4\pi}\right]$$

where $B_{(\sigma)}$ is the luminosity in the aperture plane, σ_0 is the emission frequency.

Function $\Phi(\gamma, \sigma_0)$ is a Fourier-type triangle with the center on a frequency of σ_0 and a width of $\delta\sigma = \sigma\frac{\Omega}{2\pi}$. Correspondingly, the limiting factor on the transmission appears as $\Omega_0 = \frac{2\pi}{R}$. In works [1, 8] it is shown that R and Ω related to these correlations is an optimal one. If we characterize the

quantity of the spectral-apparatus in the terms of transmissions and resolutions by factors of B = IR (where I is the input flow, R is the resolution capability), then it is possible to make a comparison of the Fourier spectrometer with a diffractionary one or a prismatic instrument in optimal conditions [9].

$$\frac{\beta_{\text{фурье}}}{\beta_{\text{дифр.}}} = \frac{2\pi f}{e} \qquad (8)$$

where f, e is the focal distance of the collimator and the aperture height in the usual spectrometer.

e) Relation of signal to the sound in the spectrum.

Let us consider that the basic source of the sound is the emission receiver, not studying, at this time, sounds connected with the emission source [10] and sounds calculating the interferogram composition [9]. If the sound in the receiver carries a thermic character, which is normal for a majority of bolometers, then the relation of the signal to the sound in the spectrum will be equal to [11].

$$\frac{s}{n}(\sigma) = \sqrt{2\tau}\,\Omega S\,(\sigma)\,\frac{B(\sigma)\,\delta\sigma}{q}\sqrt{T} \qquad (9)$$

where $B_{(\sigma)}$/w/cm^2 $\cdot$cm^{-1} strad/luminosity of the source in a frequency σ; $\delta\sigma$ (cm^{-1}) is the resolution threshold of the Fourier spectrometer; ΩS is the geometric factor; $Q[BT/2\Delta^{\frac{1}{2}}]$ is the threshold sensitivity of the receiver; $K(\sigma)$ is passage coefficient of the instrument in the frequency; T is recording time of the interferogram. The analogous correlation for the scanning spectrometer

$$\frac{s}{n}(\sigma) = \Omega S\,\frac{\kappa(\sigma)\,B(\sigma)\,\delta\sigma}{q\sqrt{\Delta f}} = \sqrt{2\pi}\,\Omega S\,\frac{\kappa(\sigma)B(\sigma)\,\delta\sigma}{q}\sqrt{\frac{T}{N}}$$

where Δf is the amplifier band-pass, N is the number of spectral elements. With the same transmissions, the recording time of the spectrum, resolution capability and spectral passage is more favorable in the Fourier spectrometer than in comparison with diffractionary ones in relation to the signal and to the sound in the spectrum are equal to $\sqrt{N}$.

With equal areas of the cross-section of the collimator, the recording time of the spectrum, resolution capability and spectral passage, taking into consideration (8) we obtain $\frac{2\pi f}{e}\sqrt{N}$ (10)

f) Dynamic Range.

Correlation (9) is expedient for the conducting of evaluation with a selection of constructive parameters of the instrument; apertures, width of the slits, recording time and others with a given luminosity source. The selection of a dynamic range of the apparatus and the evaluation of average accuracy of the spectrum in the interferogram may be conducted from the following correlations

$$\frac{\bar{S}}{\sqrt{\bar{n}_s^2}} = \sqrt{\frac{\Delta\sigma_n}{\Delta\sigma_s}} \cdot \frac{I_0}{\sqrt{n_i^2}\sqrt{N}} \qquad (11)$$

where S is the average energy by the spectrum, N is the number of elements in the spectrum, $\bar{n}_i^2$, $\bar{n}_s^2$ is a set aside to the single interval of the abscissa axis of the root mean square of the sound value in the interferogram and the spectrum correspondingly.

I_0 is the amplitude of the central band in the interferogram,

ΔS is the general width of the optical spectrum,

$\Delta\sigma_n$ is the general width of the noise spectrum.

Formula (9) is easily obtained from (11) if in the latter, there is a change made $\Delta\sigma_n = \frac{1}{h}$, where h is the interval between calculations in the interferogram.

$$\Delta\sigma_s = .\sqrt{\delta\sigma}$$

$$I = K(\sigma)B(\sigma)N\delta\sigma$$

$$\sqrt{\bar{n}_i^2} = a\sqrt{\frac{M}{2\pi T}}$$

where M is a number of measurements in the interferogram, T/M is the time constant of the receiver-amplifier system and considering that

$$h = \frac{\chi_{max}}{M} = \frac{1}{M\delta\sigma}$$

III. GRATING-TYPE INFRARED FOURIER SPECTROMETER (BIGS-1)

The grating-type infrared Fourier spectrometer represents a complex optic-electromechanical instrument. The basis of the optical part of the instrument is composed of a Michaelson interferometer, an electronic low inertia non-cooled bolometer with a transistorized amplifier and a system of automatic control, a mechanical-pitch driving gear of a mobile interferometer mirror and the construction design of the light-divider.

1) Interferogram recording of low-temperature emission sources.

The recording of emission sources having a temperature lower than the receiver temperature is very significant with the study of Earth spectrum emission and that of several other planets, when as receivers are served. non-cooled bolometers having a temperature of 300° K.

One has three methods of recording similar emissions.

a) A rapid scanning of the interference band and in this manner of ampligying the modulated signal.

The signal in the receiver will consist of two parts

$$\Phi(\gamma) = \int_{\Delta_1\sigma} Z(\sigma)(1+\cos 2\pi\sigma\gamma)\,d\gamma - \int_{\Delta_2\sigma} Z(\sigma)(1+\cos 2\pi\sigma\gamma)\,d\gamma$$

where $\Delta_1\sigma$, $\Delta_2\sigma$ correspond to the frequency intervals in which the temperature of the source is more (less) than the temperature of the receiver. Bands which correspond to the indicated frequency intervals are shifted in phase by 180° in relation to each other. The interferogram formed may substantially differ from the usual one: the amplitude of the central bands depending on the rate of the above indicated parts may be equal to 0, or change the signs in relation to the mean level of the interferogram. With this, the "zero" of the spectrum is "tied" to the emission curve of the receiver. For obtaining a real spectrum of the source it is necessary to add a Fourier-type interferogram to the emission curve. The signal from the source is modulated by a breaker which is found in the temperature level of the instrument. In this case, the temperature of the source is compared to the modulator temperature. In the difference of the proceding case, for obtaining phase information concerning the interferogram, it is necessary to have a phase-sensitive system of signal amplification. If the modulator is situated directly after the initial aperture of the instrument, then "zero" of the spectrum will be related to the emission curve of the modulator with a calculation of the spectral passage of the instrument.

The emission source is compared with the signal of the body at zero (or near zero) temperature in each modulation period.

The central band of the interferogram corresponds to the integral flow from the source, all harmonics of the interferogram coincide in phase and the results obtained by the Fourier conversion, the spectrum appears as a real spectrum of the source without considering the spectral passage of the instrument.

If the purpose of the experiment is obtaining the absolute spectral intensity, then with the implementation of the first two methods, it is necessary to know the temperature of the receiver or the modulator at the moment of interferogram recording. Under flight conditions on board a satellite, temperature of the instrument may change in wide ranges. This condition increases the requirement for the dynamic range of the recorder and requires a complementary arrangement for the measurement with sufficient accuracy of the temperature of the modulator and receiver.

Noting the above mentioned method, we found it expedient to utilize a third method of recording the interferogram, which was used in the basic arrangement of the BIFS-1 instrument. This differential method was first used in Fourier spectroscopy. The first of the studied methods was used earlier in [5] for recording the emission spectrum of Earth from a satellite.

2) Impulse scanning of the interferogram.

The differential method of recording the emissions requires utilization of a modulation principle, when in each period of modulation there occurs a comparison of the measured and the standard emission flow. In our case, the bringing of the interferometer mirrors and the modulator was achieved with the aid of pitch motors. In this case, the modulator was a mirror which could be placed in several positions, corresponding to the sighting of the standard and the measured emission source, while the mobile mirror of the interferometer was transferred by linear degrees from one position to the other in the process of the motion difference change.

The computation of the amplitude impulses emerging as a result of modulation is conducted in a synchronous manner by a corresponding instrument (for example, a numeral voltometer).

Principle schematics of the BIFS-1 instrument.

Let us examine the principle schematic of the BIFS-1 apparatus, consisting of optical and electrical parts. In fig. 3 there is represented an optical-kinematic diagram of the instrument. In the focal plane of the collimator mirror with a diameter of 40 mm and a focal distance of 300 mm are situated 2 input diaphragms, S_1, S_2 with dimensions of 22.5 mm X 4 mm. Diaphragm S_2 is illuminated by the examined source while diaphragm S_1 is illuminated by a comparison source. Between the diaphragms and the collimator in the axis of the pitch motor SHDM is situated a modulating mirror. Collimator K forms a parallel beam which falls on the light-divider of the interferometer at an angle of 30°. After passing the interferometer, the emission is focused on the receiver platform of the bolometer with objective O, diameter 45 mm and a focal distance of 40 mm. In the central portion of the objective which is shaded by the receiver, there is an aperture for the beam from the calibrating source which is a lamp of N incandescence. The filament of the bulb with the aid of lens L, flat mirror Z on the other side of the modulator and rotating mirror Z_3 to which the objective is projected onto the platform of the receiver. In this way the signal from the calibrated source is then a modulated frequency of the modulated signal from the examined objective. The calibrated signals of the bulb, in essence, serves as the control of the full amplification and sensitivity of the entire receiver-amplifier apparatus.

The optical portion of the instrument is not controlled. In case of necessity however, such control can be easily achieved by an automatic introduction into the channel of the measured flow by a darkened screen at the time of recording of one interoferogram for each 5 - 10 interferograms of the studied objective. Naturally, accurate measurements of the screen temperature should be kept in parallel with the activity.

In fig. 4 is presented a schematic diagram of the apparatus. As seen, the electronic portion consists of two basic points: a measuring device and systems

for control and automation. In the basis of the measuring device there is a transistorized schematic for the signal amplification from the bolometer on the carrier frequency with automatic bridge regulation for the unbalance of the bolometer [12]. In the capacity of a receiver there is used a low inertial bolometer from an alloy of bismuth and lead [13], joined with a regulating element according to a system developed in [12]. The bolometer has a receiving area of 3 X 0.5 mm^2, a time constant of approximately 5 millisecond and a threshold sensitivity of 10^{-10} watts/$hertz^{\frac{1}{2}}$. The amplification device includes in itself, a generator carrying power to the bolometer, an amplifier of the carrier frequency, an automatic compensating device, a detector and impulse-amplifier of low frequency. The arrangement for the power to the accumulators: the schematic for control and automation is commenced from the generator of rate impulses, whose repetition frequency is 12.5 hz. Through electronic switches, from this generator the winding of the reverse pitch motors of the modulator and scanner are supplied with power. The pitch motor of the modulator in the process of the work takes on two positions of the roller shifted to an angle of 5°. The pitch motor of interferometer mirror scanning is shifted to one side until a maximum difference is reached in the motion. Further, with the aid of contact-relay devices there is achieved a reverse and movement in the opposite direction in double rate of the maximum motion. In the moment of reverse of the relay device is decreased and simultaneously by one second Δt = 1 sec a standard bulb for calibration is switched in the circuit. The power supply for the control which also includes, in effect, relay blocks of remote switching on and off of the instrument is achieved from the grating network or from an individual accumulator. The maximal double motion difference consists of approximately 5 mm which corresponds to the resolution capability of approximately 1 cm^{-1}. One pitch transfer of the mirror is approximately 2 μm. The regulation of the contact position may be established by a double motion difference in the regions of 0.5 + 5 mm. With this the recording time changes from 40 to 400 sec. The time of signal accumulation (mirror adjustment at a given

pitch) with a selected velocity of mirror movement consists of approximately 80 msec.

IV. SPECTROMETER CONSTRUCTION

Let us examine the separate components of the BIFS-1 instrument

a) Interferometer

The basic construction of the apparatus is in the interferometer block which consists of two flat mirrors and a light-divider with corresponding mountings. The main requirement directed to the interferometer of a grating-type instrument consists of that in which its properties would not change in the presence of significant exterior action (overloading, temperature variation, pressures, etc.). Besides that, a significant value is the small weight of the instrument. For the interferometer utilized in a satellite, this problem is solved by the establishment of an interferometer construction in the guise of a duraluminum cube which carries the light-divider and the mirrors [2, 5]. The authors noted that a similar construction was twice as successful in enduring the entry into Earth orbit without disrupting the alignment. Stability against overloading was attained by rigid material and construction. Work [5] appears, obviously, as a better achievement, but even here is noted an insufficient construction rigidity in the interferometer.

Even in the BIFS-1 apparatus, the interferometer node is also constructed of a monolith milled from a whole section of metal. However, in the capacity of a monolith material, an alloy of aluminum magnesium was selected, (ML-5 brand) possessing a much higher rigidity than the usual duraluminum. The interferometer block is fastened on the plate of this material. The plate supports the area where the collimator and the focusing mirrors, the receiver and the modulator are positioned. Below the plate is fastened a hermatical electronic block. The fulfillment of basic requests of apparatus construction from the ML-5 alloy also has another advantage, there specific gravity of this material is almost $\frac{1}{2}$ times less than duraluminum.

The stationary mirror of the interferometer is secured and is a basic point

of alignment for the interferometer. For this purpose, it is fastened to a special mount, having in the center a steel collar which is rigidly connected with the monolith (Z_2 in fig. 3). The alignment in the two planes is achieved at the expense of elastic deformation of the collar by a pair of screws in corresponding planes.

The mobile mirror of the interferometer connected with the change mechanism in the motion difference (Z_1 in fig. 3) is fixed to a four-faced prism from steel alloys the brand of KhVG. The side and lower surfaces of the prism are polished with an inclination from the plane by no more than 2 rings in visible light (the ridge angle does not exceed 5 sec). The prism is held by metallic parts in a thin layer of polyfluoroethylene resin -4. This insures a friction with a coefficient of 0.02 without the utilization of liquid lubricants. The prism is brought into movement by the micrometer screw. Its pressure to the screw push rod (and movement in the opposite direction) is insured by a spring. The micrometer screw turns with a corresponding pinion pair of pitch motor MSHR-2A. Each pitch motor functions with an accuracy of $\pm$ 2% in a 5° angle. This corresponds to a prism shift by 1 μm.

In fig. 3 are seen end contacts (1 and 2) whose locking which occurs with the screw shift of the michrometer brings about a reverse in the pitch motor.

The utilization of the pitch motor in MShR has a number of advantages in relation to the construction aspect. Since the size of the pitch motor does not depend on the load moment, this is rather important for it excludes the influence of friction skips with a fixation of the mirror position. A similar system gives the possibility of interrupting the recordings. It is necessary to note that the optical portion of the instrument is not hermatized and in this way can function under conditions of low pressure. This is why the mobile parts of the pitch modulator and the pinion pair is treated with sulfromolybdedum lubricants which insure a normal function of the comparatively slow moving elements during a long period of time even under conditions of high vacuum [14]. In the capacity of a light-divider in the interferometer of the BIFS-1 instrument a film from terrylene

with a thickness of approximately 6 micron is utilized. The use of this film is favorable for this spectrum region since the transparent crystal the type of KVr or CSJ are very hygroscopic. This terrylene film in the working range of the spectrum region has a refractive index of n = 1.85 and an insignificant quantity of absorption bands (see fig. 5). A study of the spectrum reflection showed that in portions where the bands are absent, the absorption in the film was practically not observed. In this way, the quantity of the reflective coefficient R in the working region in the working range consists of 20 - 30%. It is known that the effectiveness of the light-divider η, that is, the interferometer passage with a zero motion difference consists of $\eta = 4RT$. Consequently, in our case the quantity $\eta = 75\%$. The significant dimension in the refractive index of the film with its given thickness brings about a selective decrease in the passage due to interference effects in the film. Actually these effects may be calculated by Frenel as variations η, which was accomplished in [15]:

$$\eta = \frac{8RT^2(1-\cos\delta)}{(1+R^2-2R\cos\delta)^2}$$

where $\delta = 4\pi n\sigma d\cos\theta$, and θ is the angle of incidence of the beam on the film. In work [16] it is snowh that for film with n = 1.85 and a thickness of 6 μm, the minimum passage is distributed in $\sigma = 500$ cm^{-1}. In a series of cases the presence of this minimum played a positive role. Specifically, with the study of the atmospheric absorption spectrum, an important role was played by the problem of dynamic range, it was an increase of relative passage in the long-wave region of the rotating spectrum pair (250 - 400 cm^{-1}) and in the short-wave region of the spectrum of CO_2 (600 - 700 cm^{-1}). A similar passage structure meliorated the dynamic range of the instrument. A theoretical calculation and the verification of the film passage from the terrylene in the interferometer achieved by us in the schematic in conjunction with spectrometer IKS-12, allowed us to construct the passage curve of the Fourier Spectrometer in the working range of the spectrum. This curve (4) is shown in fig. 6. Here is presented the interference

curve in the film (2) and the passage of selective elements in the optical schematic of the Fourier spectrometer (1). From the long-wave edge of the spectrum the limiting is achieved by an aperture of the bolometer from the KRS-5 crystal and from the short-wave edge by dulling the collimator of the mirror and changing the mirror of the modulator with a polished crystal.

A significant value for the quality of the interferometer is the fasterning of the film. In our case the film was stretched on the mounting ring from alloy steel with a KHVG brand with a special regime of thermal process. The flatness of the ring laying on the film is contained with the accuracy of one band in visible light. The mount together with the film is fastened to the monolith of the interferometer at three points. In the fastening system there is noted a deformation compensation of the mount due to various temperature coefficients of steel expansion and our alloy ML-5.

b) Electronic Assembly

The electronic system in BIGS-1 insures the signal amplification in the bolometer (measuring device) and control and conductance of electromechanical nodes. The electronic assembly located in a hermatic case to exclude the influence of pressure changes on the function of capacators, accumulators and other elements.

The measuring device includes a generator carrying the bolometric bridge, a carrier amplifier, detector, automatic compensating device, a low frequency impulse-amplifier and economic bulbs of the rod type.

The power supply for the measuring arrangement (except the impulse-amplifier) was achieved from accumulator batteries through a usual pressure stabilizer. Automatic power supply of the first cascade of the amplifier allows a reliable omission of electric interference, entering the measuring device from the general power plant network and to realize the threshold sensitivity of the bolometer, also, the supply of the impulse-amplifier from the electronic pressure converter also working from the pressure stabilizer.

To increase the economical operation of the instrument, the impulse current in the windings of the pitch motor is conducted with a considerable gap. For reliable function of the motors it was sufficient to have the gap at 1:5. The entire schematic functions reliably in the temperature interval of -40° C.

V. INTERFEROGRAM RECORDING

a) Recording and processing the interferogram.

The recording of the interferogram by the BIGS-1 instrument with satellite application was achieved with the aid of telemetry systems. In this case, the system must synchronize the generator schematics of instrument control so that the computed indications would occur at a certain moment upon reaching the impulse of the output signal at its maximal value. In certain cases, (for example, in aircraft or balloon) and also with the exploitation of the instruments in near-earth conditions, the recording is made on a perforated tape. With this, the recorder switches in a fast acting numerical volt meter VK7-10 with 3,000th division and an internal start, with a PL-20-2 perforator with 8 dual-channels and a transition schematic with a start-up and delay design (fig. 7).

The schematics of interferogram recording function in the following manner. Signals from each of the dual output numerical light meters through the designated cascades 1 - 8 (fig. 7) are channeled to the output of the preamplifier coding the electromagnetic perforators EM-1 + EM-8. The start-up of the numeral voltometer is made by the impulse of the rate generator. In the interval of time ΔT = 15 msec after pressure measurement necessary for the establishment of the coding electromagnetic perforator, with the impulse input into the input of the preamplifier controlling the electromagnetic EM-9, there occurs a perforation of the tape. Delay time is insured by the single vibrator of the delay period.

Prior to further processing of the interferogram on the IBM, it is sometimes necessary to evaluate the quality of the recording and selection of the interferogram. For this purpose we have constructed a device to compute the perforated

tape, which achieves the transfer of the dual code of the tape into a proportional signal and records it on an automatic recorder the type of EPP-09 (the time of recording, three second-points).

In fig. 8 there is presented an emission interferogram of an absolute black body at room temperature which was recorded on a perforated tape with a subsequent record on an EPP-09 tape. The described device provides the possibility for a direct introduction of the interferogram into the IBM from the perforated tape, and also the evaluation of the perforation quality and the selection of the interferogram for further processing.

b) The processing of the interferogram (obtaining the spectrum).

The solution of the Fourier integral [5] for obtaining the spectrum from the interferogram is made on the IBM. In our work BESM-4 computer or M-20 were utilized.

In the process of solution the total was calculated

$$B(\sigma_i) = \frac{1}{N} \sum_{n=0}^{N-1} A(n,N) \Phi(n,h_\gamma) \cos 2\pi \sigma_i n h_\gamma$$

where h_γ is the interval by the motion difference between points of measurement of the interferogram. Functi$\Phi(n,h_\gamma) = S(\gamma) - \Phi_o$ insured the assignment of preliminary numerical material. Also assigned were a number of points N, pitch dimensions h_γ, frequency interval h_σ equal to $\sigma_i - \sigma_{i-1}$ and boundary frequency of the spectrum that was of interest to us σ_{min}, σ_{max}. Pitch h_σ was assigned on the basis of the required number of functions $B(\sigma)$ on the resolution interval of the spectrum. Value Φ_0 was computed automatically in the process of solving the problem.

In the process of programming there were certain introductions of "apodization." "Apodization" was performed by multiplying functions $\Phi(n, h_\gamma)$ on a triangular adjusting function $A(n,N) = 1 - n/N$. This operation substantially decreased the variation caused by secondary maximums of the apparatus function without any substantial decrease in resolution. In fig. 2 there is shown an apparatus without "apodization" and an apparatus function with a triangular one. Fig. 9 illustrates

the influence of "apodization." Here is presented a spectrum of an absolute black body at room temperature without "apodization" (oscillating curve) and after introduction of apodization (dotted curve).

The results of IBM calculations were introduced into a numerical printer.

VI. DETERMINATION OF THE CHARACTERISTICS AND TESTS OF THE BIGS-1 INSTRUMENT

In fig. 10 there is shown a general view of the grating-type Fourier spectrometer BIFS-1 with the upper lid removed. In fig. 11 is shown a laboratory, measuring complex consisting of the BIFS-1 apparatus, the numerical volt meter the type of VK7-10, and a perforator the type of PL-20-2. Finally, in fig. 12 is presented a photograph of the code-analog converter and potentiometer recording the interferogram.

This constructed apparatus permits the recording of emission spectrum (or transmissions) in regions of 10 μm to 40 mm. The relation of the signal-sound in the interferogram for the emission spectrum of an absolute black body at a temperature of 290° is equal to ~100 (by the maximum of sound elimination). In this way, the signal equal to the sound is reached with the temperature of the emitter at ~90° K (for average quadratic sounds ~60° K). For obtaining the spectrum with a determined accuracy, it is necessary that the temperature of the emission source consist of ~120 - 150° K. The theoretical resolution capability of the instrument at minimal is 10 cm^{-1} and at maximal is 1 cm^{-1}. The time of recording from one point in the interferogram consists of 80 msec at a pitch of 2 microns.

In this way, the recording with a resolution of 10 cm^{-1} takes 20 sec. Under these conditions the "apodization" brings about the resolution of 15 cm^{-1}.

The overall size of the instrument is 350 X 300 X 260 mm with a weight of 8.0 kg and a power usage of approximately 3 watts. The range of working temperatures is from - 40° C to +40° C.

For the determination of real spectrum characteristics of the instrument, a

series of spectrum emissions and absorption were obtained with its utilization. In fig. 13 are shown emission spectra of an absolute black body at a temperature of 290° K (calibrating signal from liquid nitrogen T = 77° K). The figure illustrates the reproduction of the instrument in ranges of 800 - 250 cm^{-1} since both of the spectra are obtained from various interferograms recorded for 20 sec (with a resolution of 15 cm^{-1}) with a peak sound in the interferogram of 1 - 2.6. In the drawing there is seen a wide minimum of approximately 530 cm^{-1}, which is related to the interference in the film of the light-divider and the absorption band of this film approximately 385 cm^{-1}. The intensity difference of the spectrum emission consists of 3 - 5%. The absorption band rate of the film in the recorded spectrum is approximately 20 cm^{-1} which characterizes the resolution of the instrument.

In fig. 14 there is presented an emission spectrum of a globar which passed through the thickness of the atmosphere of approximately 5 meters (in room conditions), obtained with the same resolution factor. Here is seen a 15 micron absorption band of CO_2.

The recording of the globar emission was also conducted for the clarification of precision determination of the zero motion difference on the spectrum outlook. In our case, with the introduction into the IBM of information after the perforator, the determination accuracy of zero motion difference was equal to 1 pitch (that is 2 microns). In fig. 15 are presented two spectrum of the globar. In one case (dotted curve) the zero motion difference is determined by the nearest point with a discreteness of 2 μm. In the other case (solid curve) the zero motion difference was determined by a construction near the zero motion difference of the interferogram by way of interpolating between two points closest to that position. The determination accuracy of the motion difference was increased to $\sim$ 0.1 micron. As seen from fig. 15, the zero line in the spectrum obtained with the undetermined position of the zero motion difference of 2 μm is shifted in relation to the more accurate curve by almost 10%. From here there is a direct

requirement determining the accuracy of the zero position of motion difference in the interferogram.

The interferogram of the emitter with a comparatively narrow spectrum is shown in fig. 16. In this case the recording of the globar emission was obtained through an interferogram filter with a width of 100 cm^{-1} which was centered in the range of 1000 cm^{-1}. The irregularity of passage and also the absorption band of the film (approximately 1020 cm^{-1}) of the light-divider determines the characteristic structure of diffraction in the variations of interferogram intensities. In fig. 17 (solid curve) there is shown the emission spectrum of the globar with this filter. This figure also illustrates the improvement of the instrument resolution capability with an increase of the motion difference in the process of the recording. In the capacity of an objective with narrow absorption lines, in this case there was selected ammonia with a pressure of $\backsim$ 40 mm col. merc. (The length of tube 100 mm.) Curve 2 relates to the absorption spectrum of ammonia (the globar-emitter with the same filter) with a resolution of 15 cm^{-1}, curve 3 with a resolution of 7.5 cm^{-1}. The absorption spectrum in a wide range is characterized in fig. 18, where the absorption is shown in the bands of trichlorobenzol (frequencies shown in fig. 6). Dotted lines indicate the spectrum of the globar. The threshold resolution is 15 cm^{-1}.

One of the most basic elements with experiments of the spectrum apparatus is the determination of the real apparatus function, determining its resolution capabilities. Certainly, the above presented spectrum in some measure illustrates the resolution capability of the instrument. However, we presented a direct experiment in the determination of the instrument function of the apparatus. The gist of the experiment consisted in that with the aid of the instrument it realized the recording of the emission lines of the laser, the width of which was quite smaller than the possible instrument function. In the capacity of such a source we used a gas laser on CO_2 $\backsim$1000 cm^{-1}. The width of the laser line emission consisted of $\backsim 10^{-2}$ cm^{-1}. In the experiments were recorded a series

of interferograms with various motions of the interferogram mirrors. In fig. 19 in the capacity of an example, are presented two recorded emission lines with a motion difference of 1 and 2 mm. As seen, the half-band of these lines in substance equalling the width of the instrument function of the apparatus consisted of 10 and 5 cm^{-1}, respectively. The processing of the interferogram was conducted with triangular apodization. A variation of the intensity near the zero line was connected with a significant level of sound in the emission of the same laser. The theoretical and experimental values should be noted, since they are determined by the conditions near the short-wave boundary of the range which verifies a good quality of the instrument function.

In conclusion, the authors consider it their duty to express their gratitude to V. A. Konyukh for the possibility of conducting the measuring with the lasers and also to Yu. A. Konyukh for the possibility of conducting the measuring with the lasers and also to Yu. S. Ivanov, A. G. Orlov and their colleagues who took part in the construction of the experimental instruments.

LEGENDS TO THE FIGURES

Fig. 1: Principle diagram of interferometer.

Fig. 2: Theoretical apparatus function of Fourier Spectrometer

Fig. 3: Optic-kinematic diagram of the apparatus

Fig. 4: Block-diagram of the Fourier spectrometer

1 Measuring device

2 Control system and automation

3 Interferometer pitch motor

4 Modulator pitch motor

Fig. 5: Spectrum transmission of the light-divider film (d = 6 micron)

Fig. 6: Spectrum transmission of the instrument

1 Transmission of selected elements of the Fourier spectrometer

2 Interference curve in the film

3 Transmission curve of the tube aperture from potassium bromide

4 Total instrument transmission curve

1 - 9 Absorption bands used with calibration

Fig. 7: Complete block-diagram of the laboratory measuring complex

Fig. 8: Emission interferogram of an absolute black body ($T = 290^{\circ}$ K), recorded on a perforator and reproduced on a potentiometer type EPP-09

Fig. 9: Apodization influence on the recorded spectrum

Solid line—processing without apodization

Dotted line—processing with apodization

Fig. 10: General view of the Fourier spectrometer type BIGS-1

Fig. 11: General view of the laboratory measuring complex

Fig. 12: General view of the code-analog converter with potentiometer type EPP-09

Fig. 13: Emission spectrum of an absolute black body ($T = 290^{\circ}$ K) with utilization of a calibrating signal from liquid nitrogen obtained at different periods of time

Fig. 14: Globar emission spectrum

Fig. 15: Influence of accuracy on determined zero motion difference

Dotted lines—certain zero motion differences with an accuracy to one pitch (2 microns)

Solid line—certain zero motion differences with the aid of interpolation (accuracy 0.1 microns)

Fig. 16: Interferogram spectrum of globar emission through a filter with a width of approximately 1 m

Fig. 17: Spectrum of globar emission which passed through the filter (curve 1) in a tube with ammonia (curve 2), resolution 15 cm^{-1}, curve 3—resolution is 7.5 cm^{-1}

Fig. 18: Globar emission spectrum which passed through a tube with trichlorobenzol

2 Real instrument function of Fourier spectrometer for 2 motion differences and a triangular apodization function

1— Motion difference 2 mm

2—Motion difference 1 mm

BIBLIOGRAPHY

1. T. Connes, "Revue d'Optique," Vol. 40, p. 45, 116, 171, 231, 1961.
2. R. Merts, "Integral Conversion in Optics," publication "Mir.", M. 1969.
3. B. A. Kiselev, Yu. D. Pushkin, "Optical-Mechanical Industry," vol. 33, No. 8, p. 468, 1966.
4. B. N. Grechushnikov, G. I. Disler, I. P. Petrov, "Kristallovrafiya," vol. 8, (3), p. 468, 1963.
5. L. B. Block, A. Zachor, "Ap. Opt", vol. 3, No. 2, p. 209, 1964.
6. R. Beer, "Journal d'Physics." vol. 28, App. to no. 3, 4, 1967.
7. "The Phys. Rad." vol. 19, 0. 418, 1958.
8. B. A. Kiselev, L. F. Parshin, "Optika i Spektroskopya," vol. 12, p. 311, 1962.
9. E. Vannase, H. Sakai, "Progress in Optics," vol. 6.
10. T. Cannes, "T. O. S. A." vol. 56 (7), p. 896, 196-
11. P. F. Paishin, "Optika i Spektroskopiya," vol. 16, p. 507, 1964.
12. Markov, M. N., Kartashev, A. V., PTE No. 4, 142, 1968.
13. Markov, M. N., "Receivers of Infrared Radiation," Publication "Nauka", M., 1968.
14. Weinstein, V. E., Troyanovskaya, G. I., "Dry Lubricants and Self-Lubricating Materials."
15. "Journal de Phys." vol. 28, addendum to Nos. 3, 4, p. 153, 1967.
16. "Journal de Phys." vol. 28, ad. to Nos. 3, 4, p. 150, 1967.

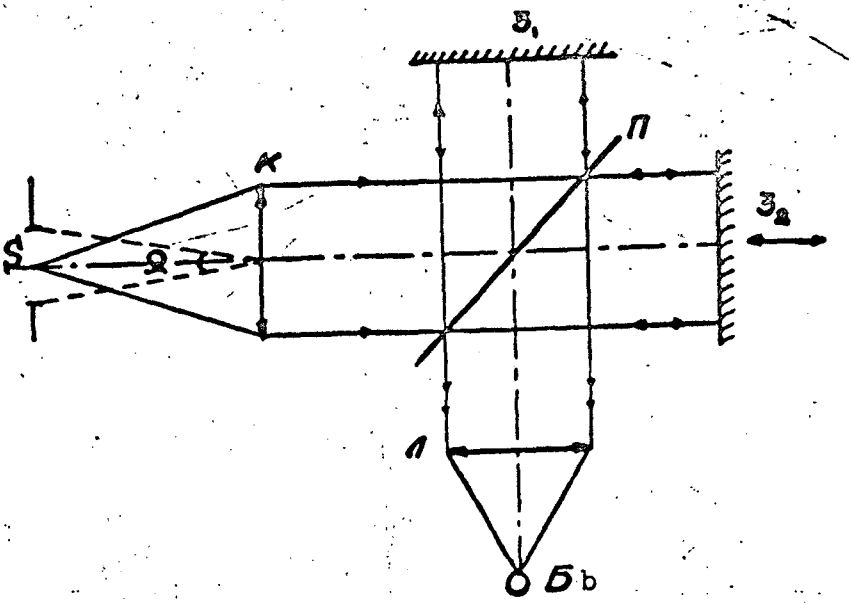

Fig. 1

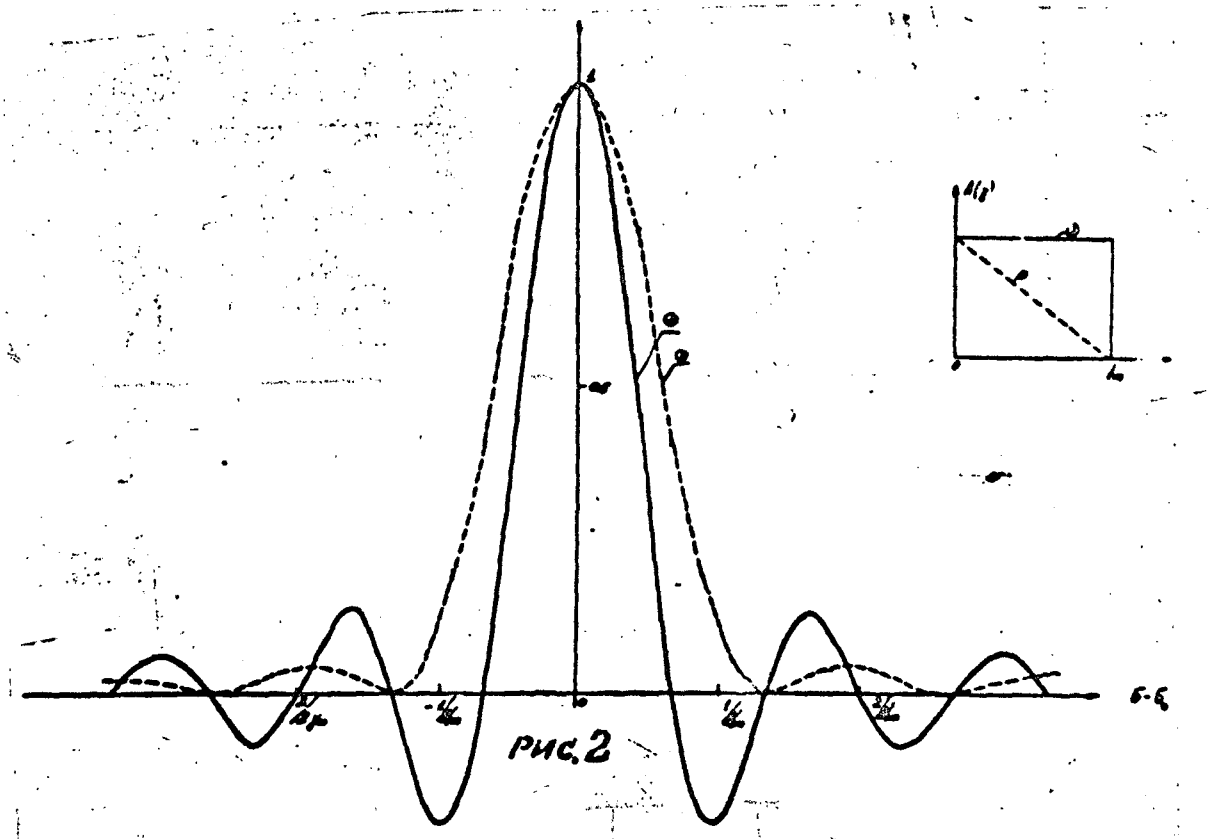

Fig. 2

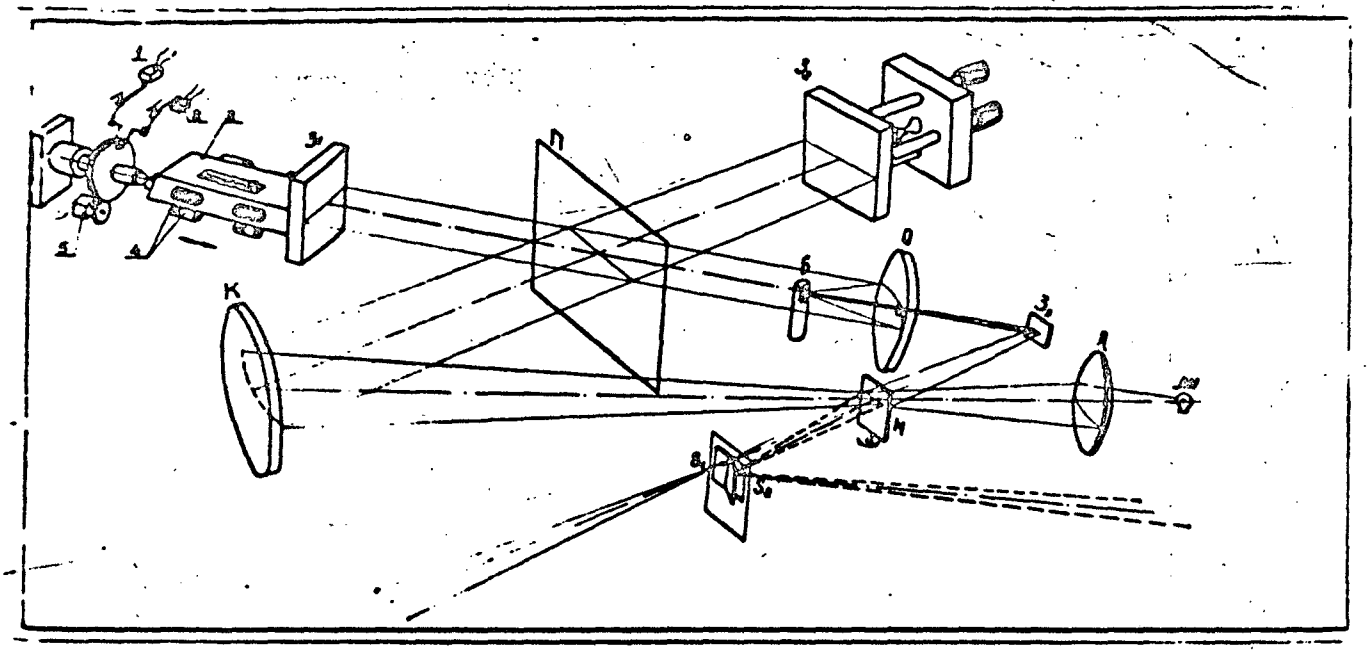

Рис.3 Fig. 3

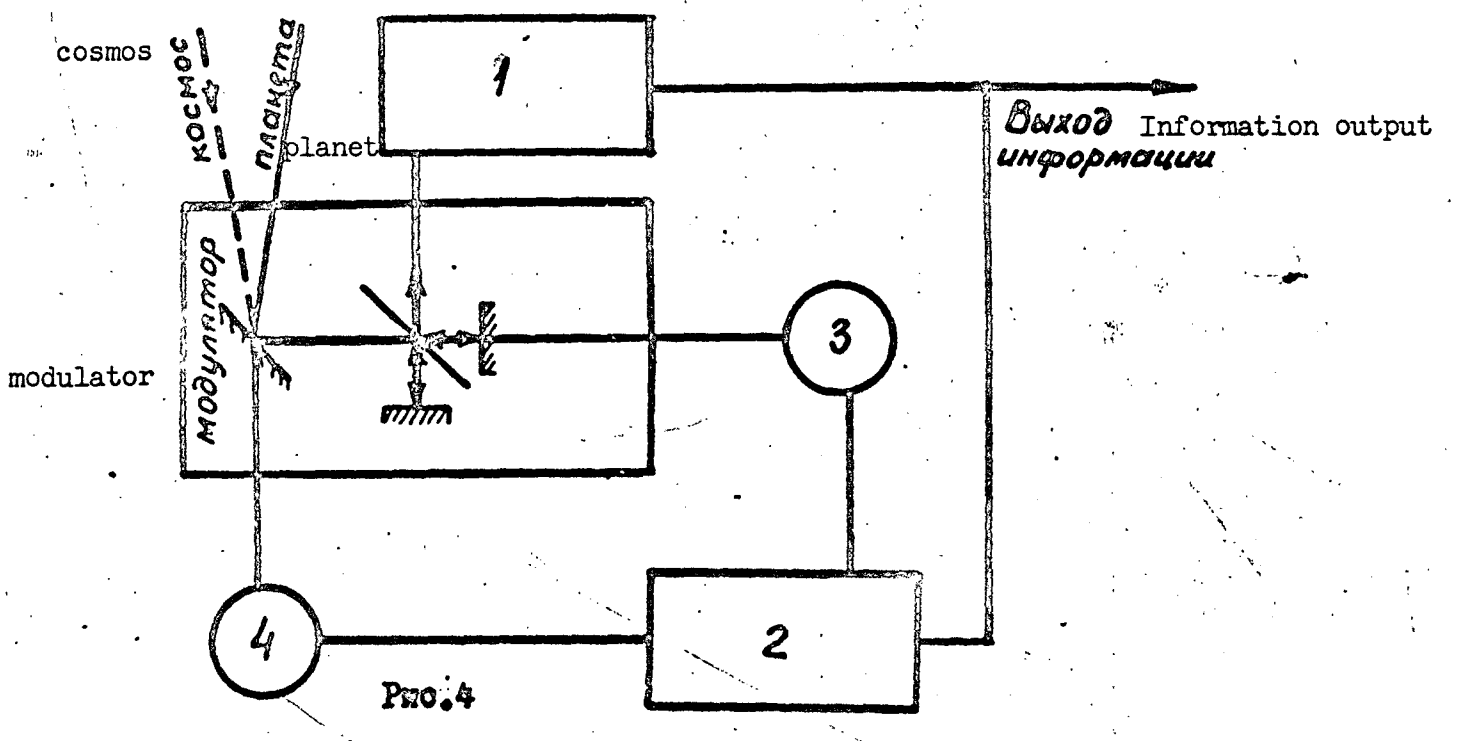

Рис.4 Fig. 4

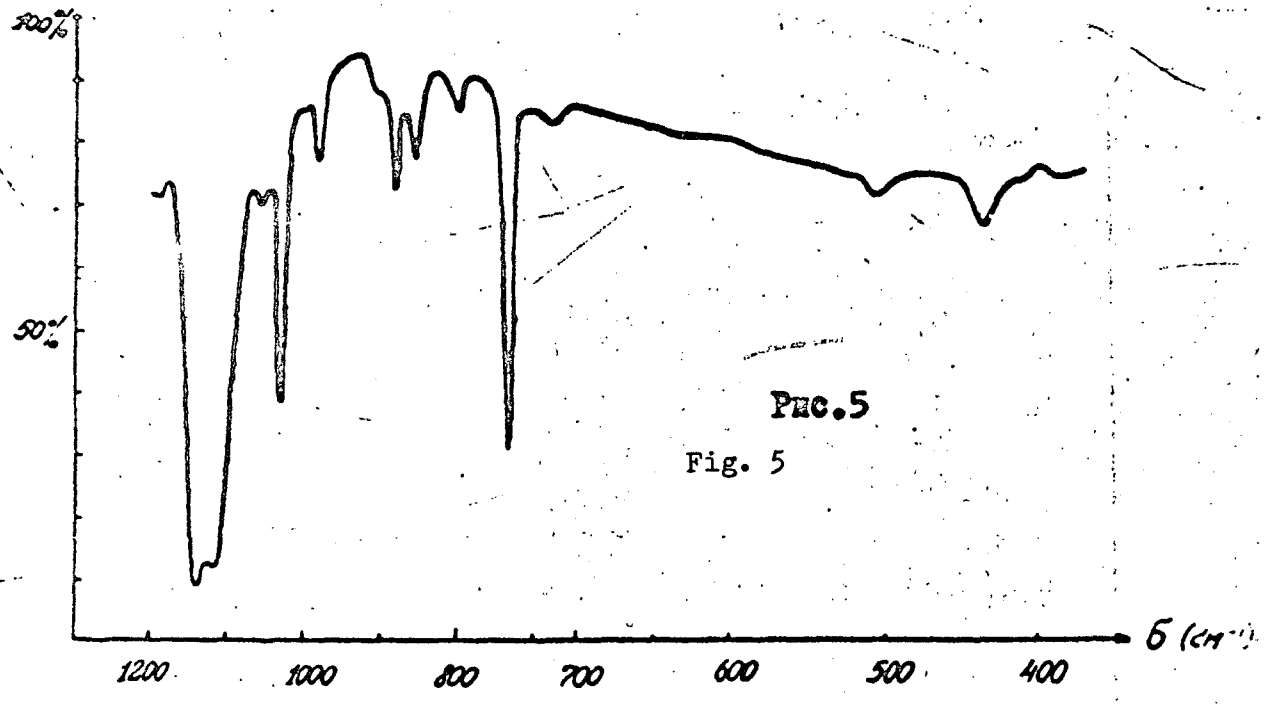

Рис.5

Fig. 5

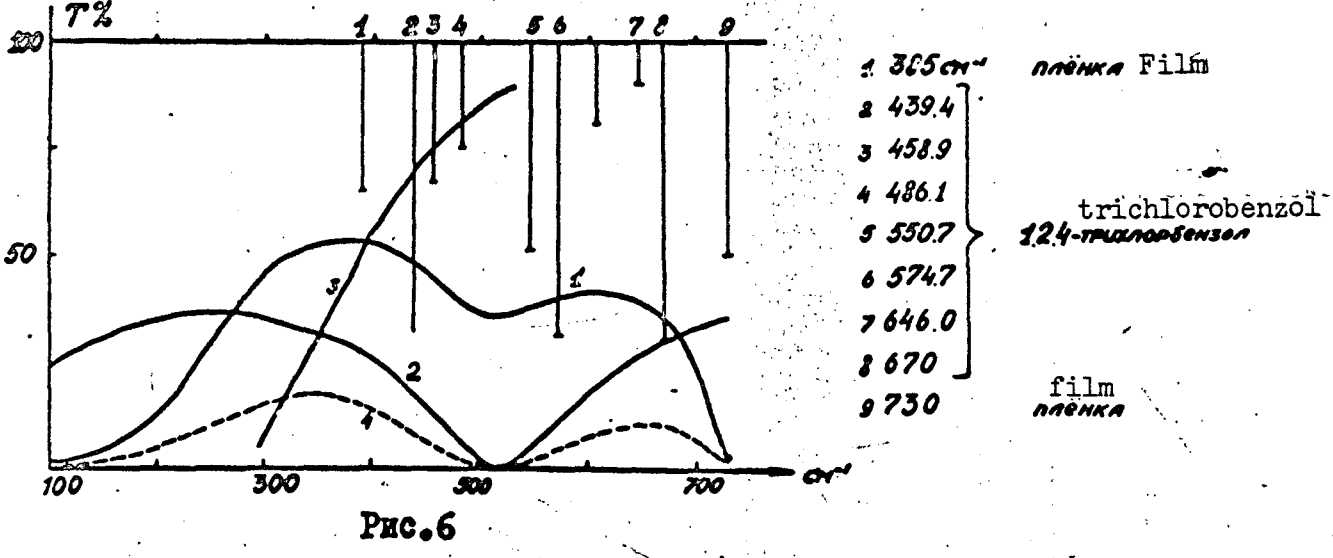

Рис.6

Fig. 6

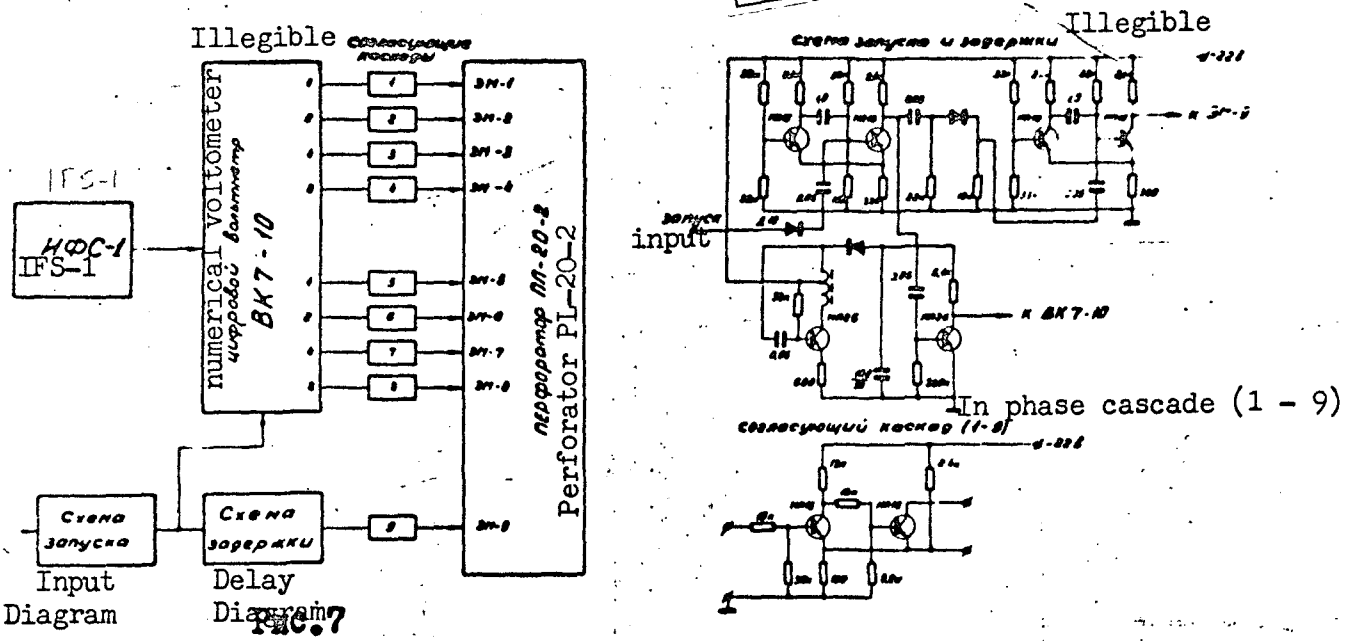

Fig. 7

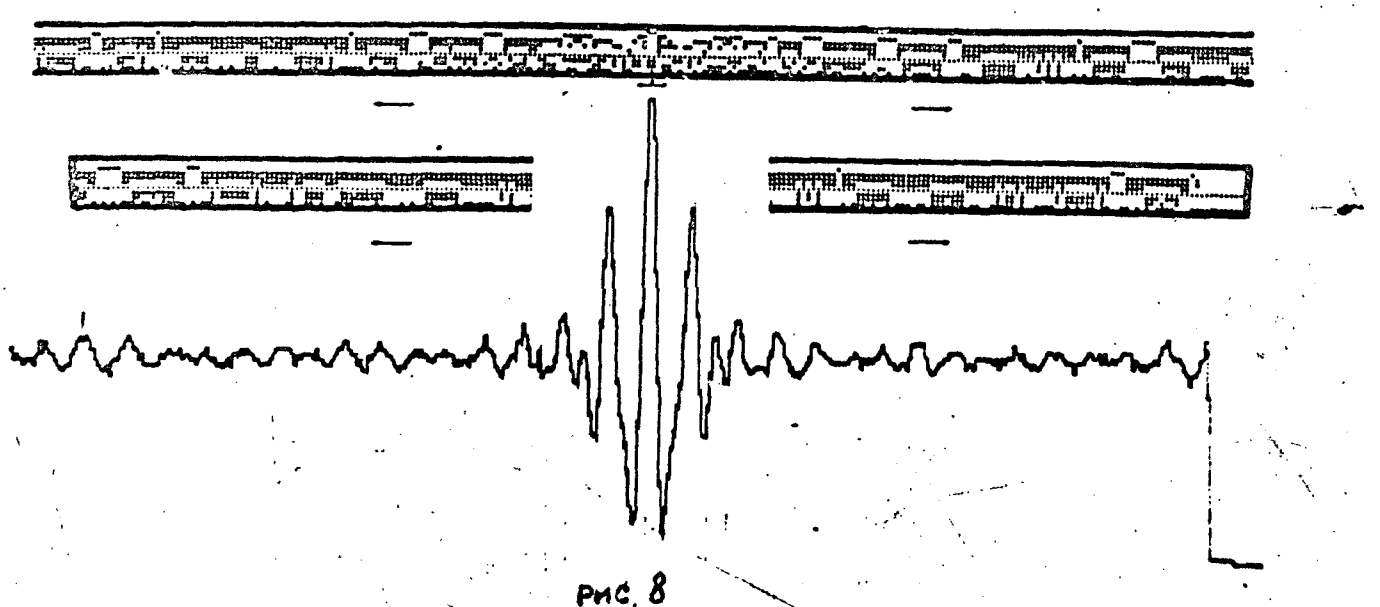

Fig. 8

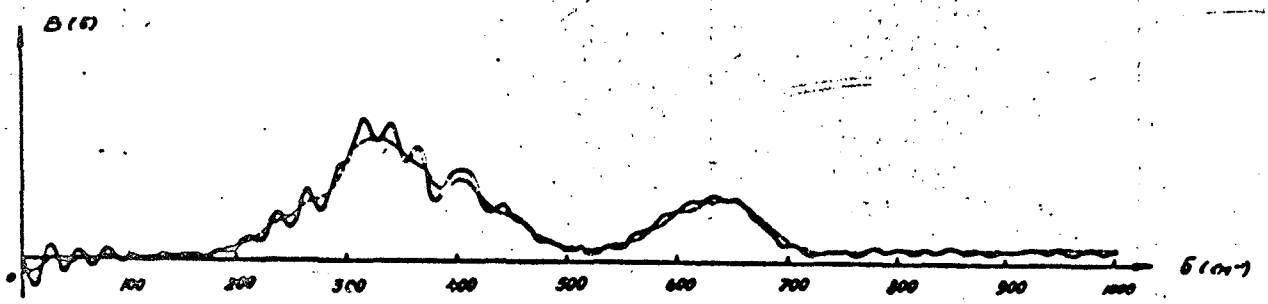

Рис.9

Fig. 9

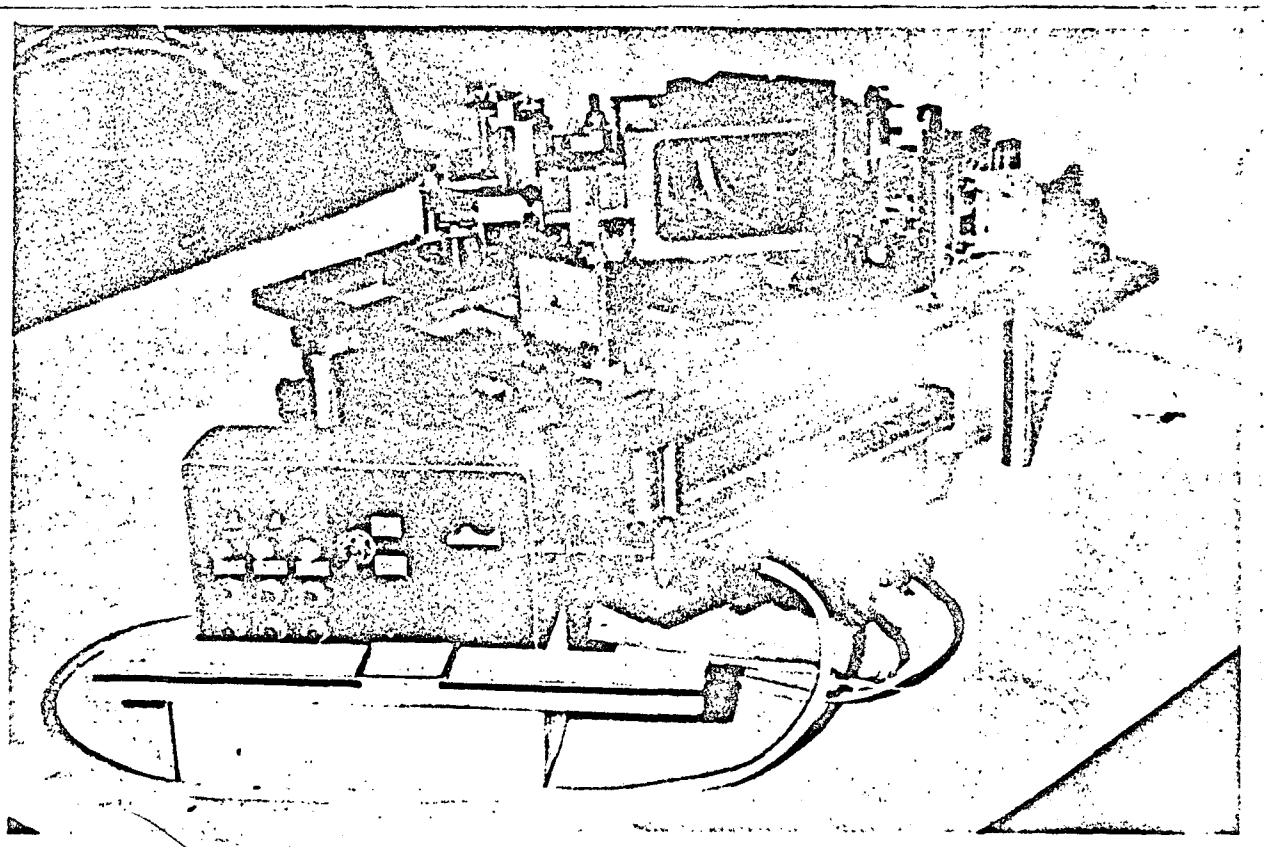

Рис.10 Fig. 10

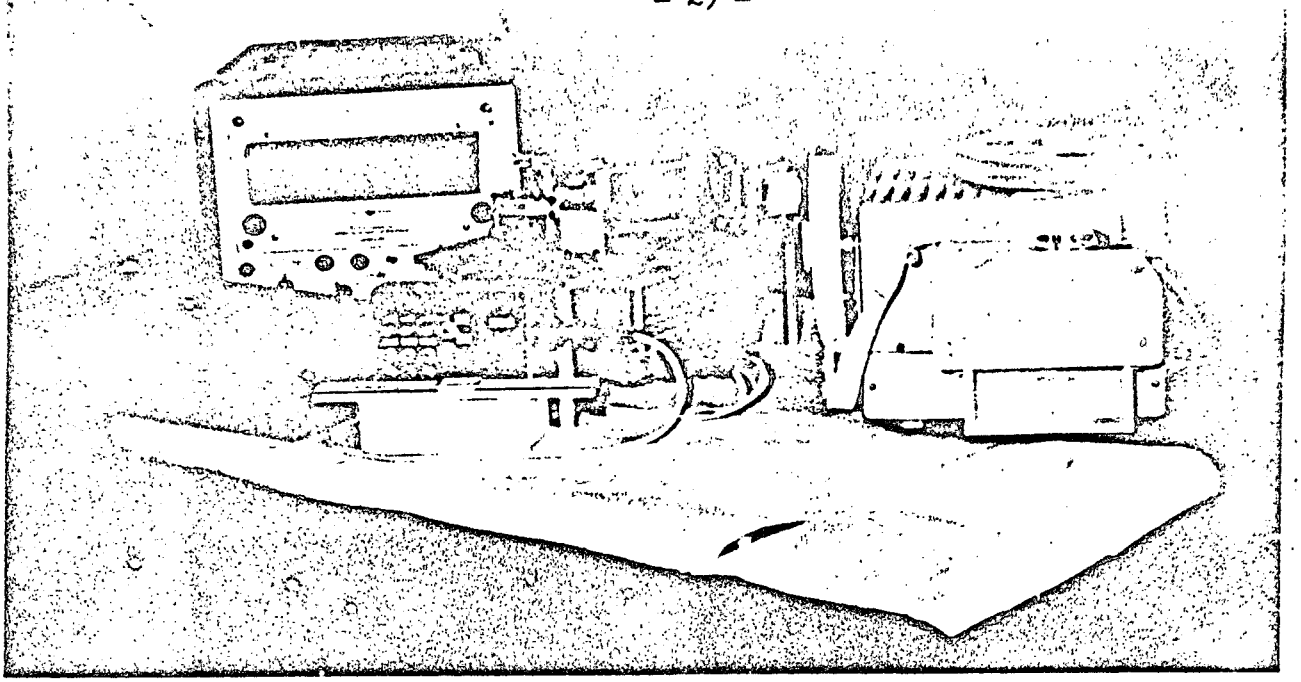

Рис. 11 Fig. 11

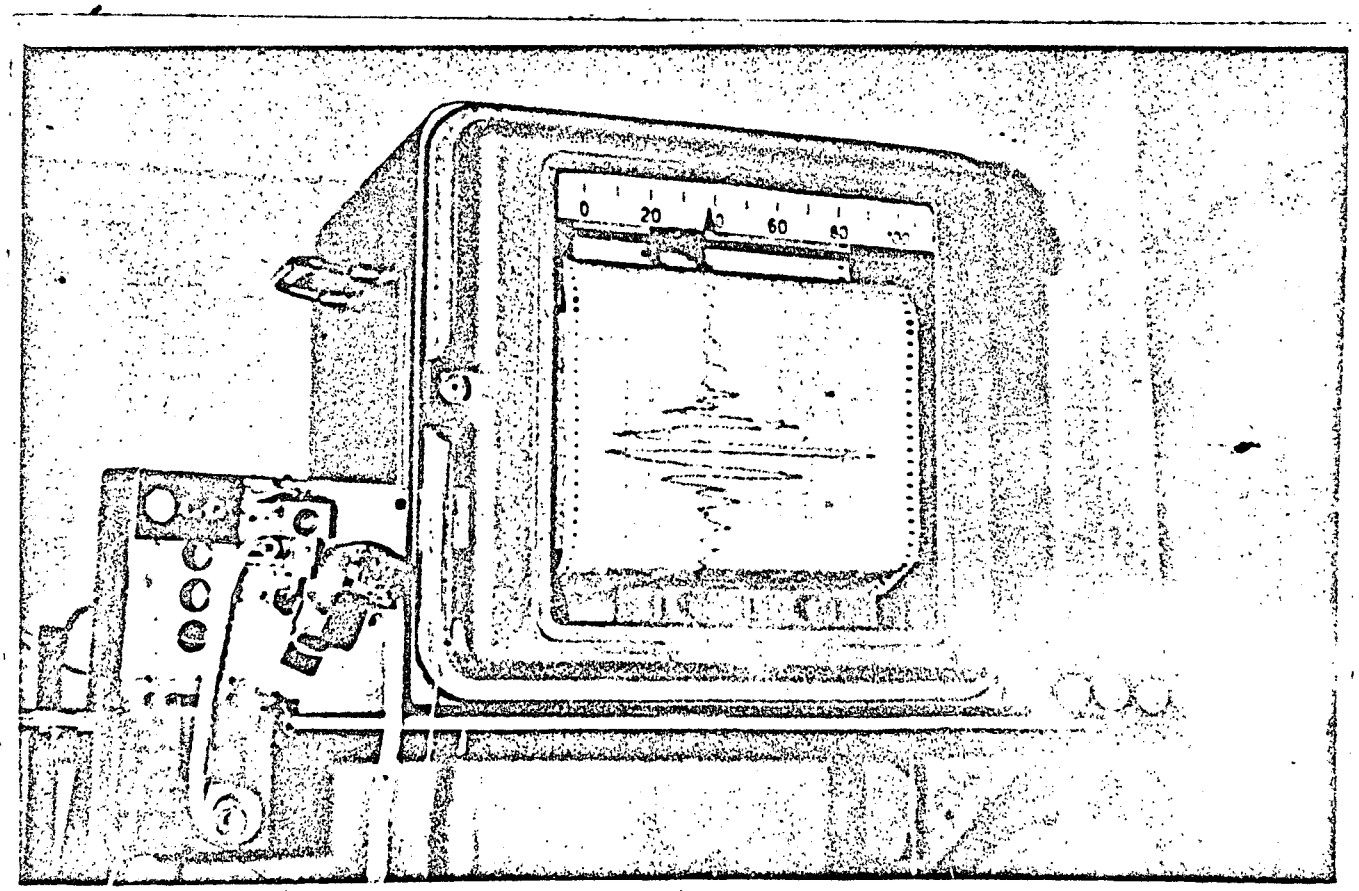

Рис. 12 Fig. 12

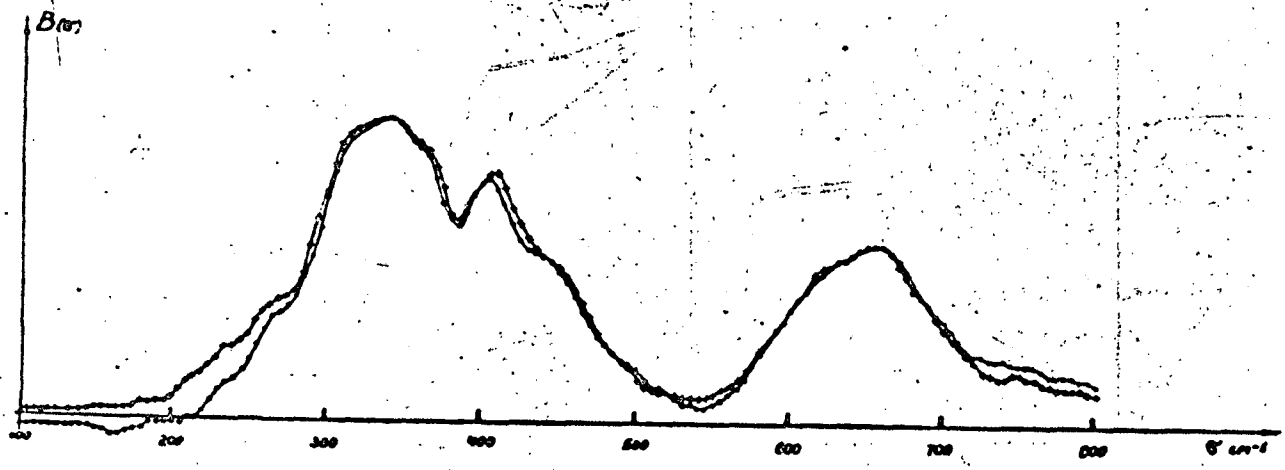

Рис.13

Fig. 13

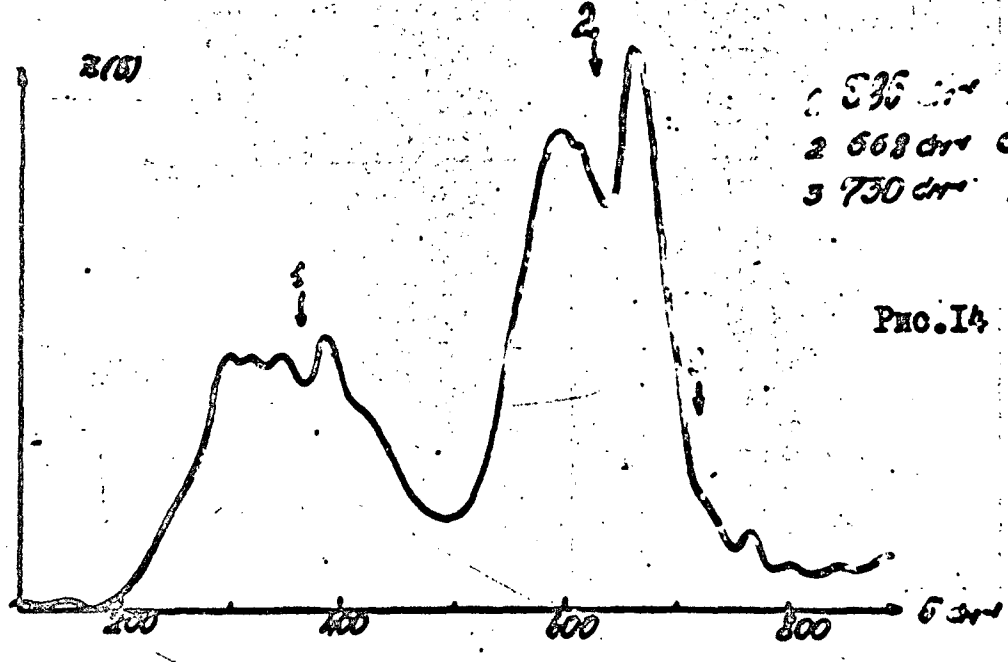

2 668 см⁻¹ CO_2 опт.

3 730 см⁻¹ плёнка film

Рис.14

Fig. 14

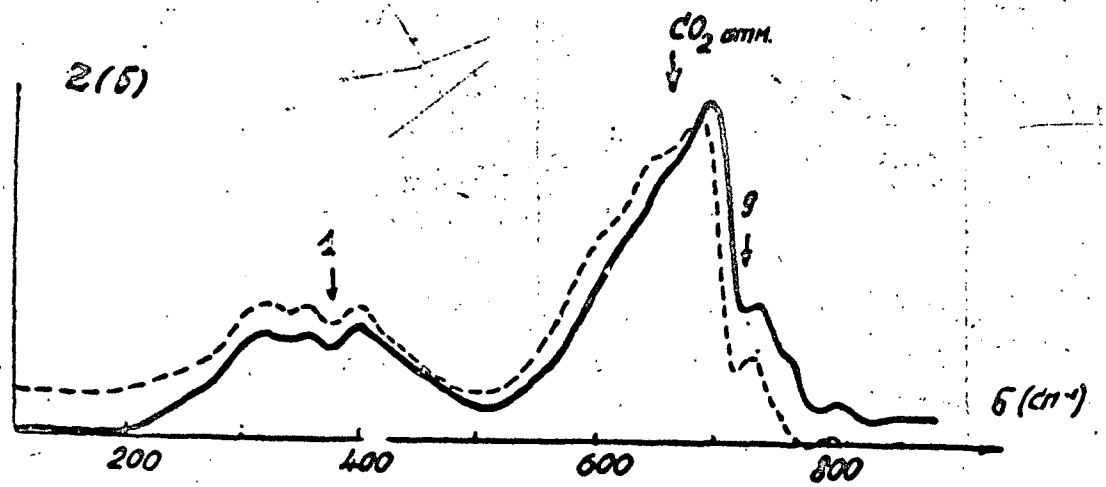

Рис.I5

Fig. 15

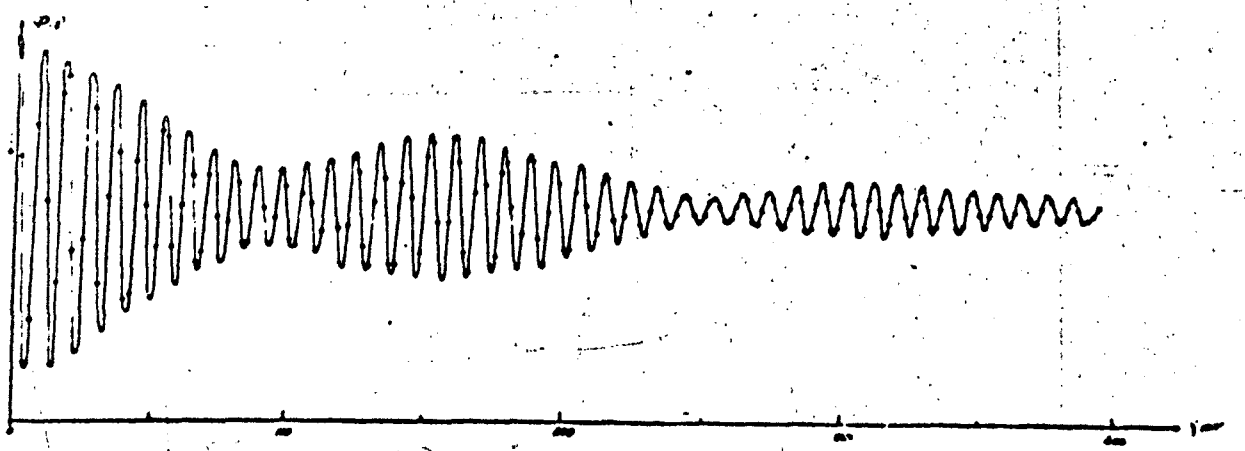

Рис.I6

Fig. 16

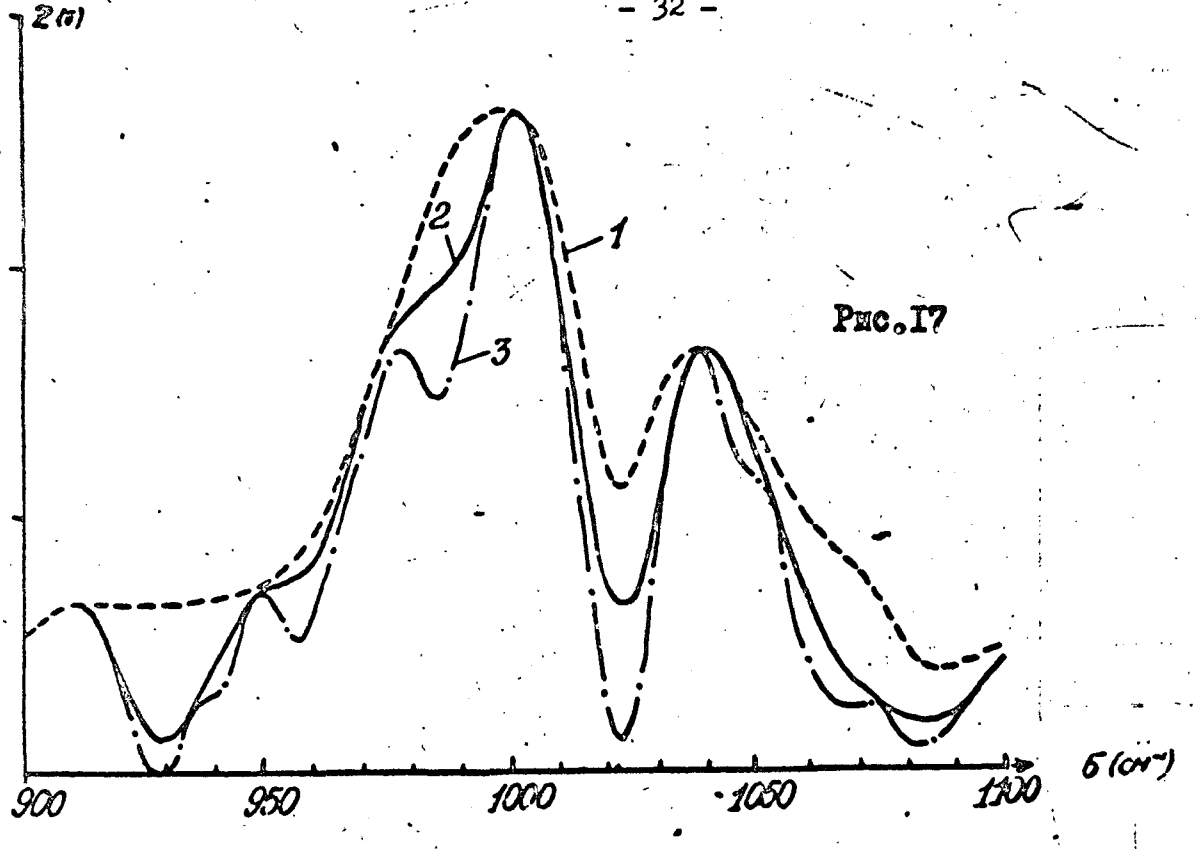

Рис.I7

Fig. 17

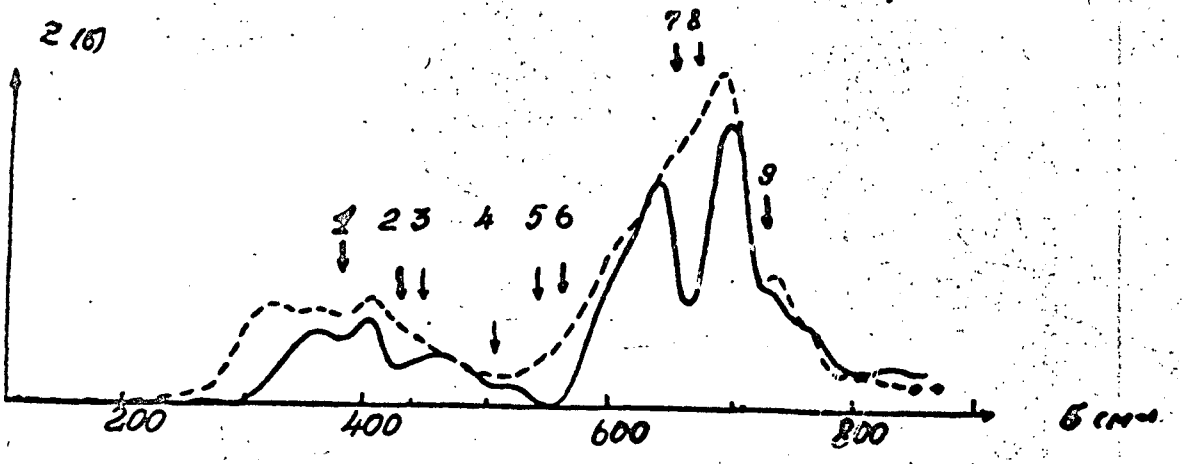

Рис.I8

Fig. 18

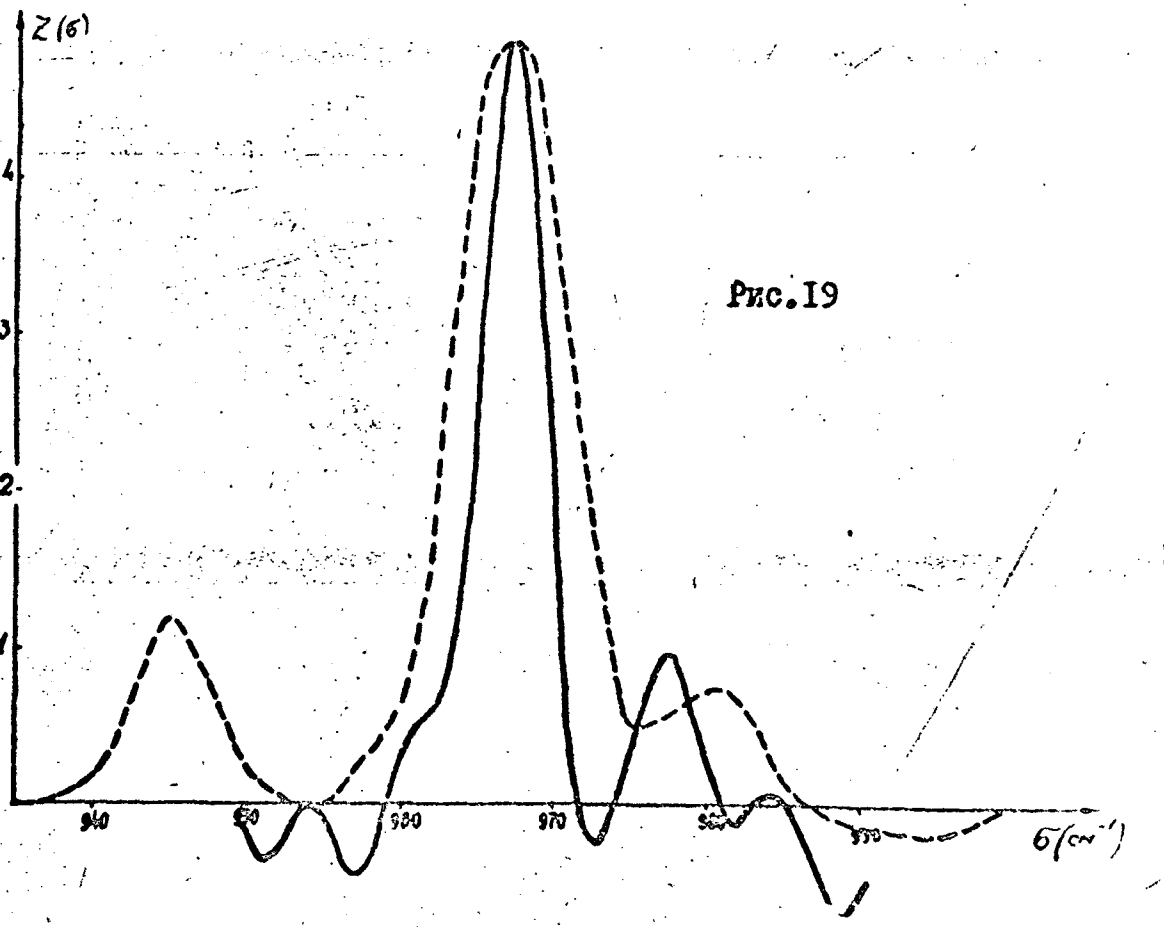

Fig. 19

Рис. I9